A NOVEL TECHNIQUE FOR REDUCING DEMOSAICING ARTIFACTS

Daniele Menon, Stefano Andriani and Giancarlo Calvagno

Dept. of Information Engineering, University of Padova
via Gradenigo 6B, 35131, Padova, Italy
phone: +39 0 49 827 7641, fax: +39 0 49 827 7699,
email: {menond, mutley, calvagno}@dei.unipd.it
web: www.dei.unipd.it

ABSTRACT

Demosaicing is the process of reconstructing the full dimension representation of an image captured by a digital camera with a color filter array. The color filter array allows for only one color measuring for each pixel and the missing two colors have to be estimated. In literature many demosaicing techniques have been proposed but the reconstructed images are affected by some visible and annoying artifacts. In this paper we propose a new effective algorithm to reduce these artifacts. This algorithm improves the performances of the demosaicing reconstruction, increasing the visual quality of the resulting images. It can be applied directly after the color interpolation, or as an off-line post-processing to improve the image provided by the digital camera.

1. INTRODUCTION

A natural color image is composed by three components, so a digital camera should be provided with at least three sensors to capture all the colors of the scene. However, this solution leads to non-simple problems in the placing of the sensors; furthermore, using three sensors is expensive and requires a lot of space.

The most common solution to this problem was proposed by Bayer [1]: a color filter array, showed in Fig. 1, is placed in front of the sensor. In this way, each pixel captures the luminance value of a given color component, for example red, green or blue, while the other two have to be reconstructed to obtain a full RGB color image. This process is called *demosaicing*.

Many techniques have been proposed for demosaicing [2]. The first ones are based on the classical methods of image interpolation, such as the nearest neighbor replication, bilinear interpolation or cubic spline interpolation. However, better results are achieved by techniques that exploit the inter-channel correlation existing between the color components. For example Cok in [3] proposed to interpolate the red-to-green and the blue-to-green ratios instead of the red and blue channels directly.

Other techniques are based on edge-directed interpolation and the reconstruction is performed along edges rather than across them. The estimation of the edge-directions is carried out using gradients [4] or other edge-classifiers [5,6].

An interesting class of demosaicing techniques interpolate the image both along horizontal and vertical directions, producing two full-resolution images. Afterwards, for each pixel, the best reconstruction is selected using suitable criteria, such as the local homogeneity of the image [7], or the consistency of the color differences [8]. Instead in [9], the two directional estimates are optimally fused using a linear minimum mean square error estimation.

G	R	G	R	G
B	G	B	G	B
G	R	G	R	G
B	G	B	G	B
G	R	G	R	G

Figure 1: Bayer pattern.

Other algorithms [10,11], after a simple interpolation, estimate the high-frequency information from the green channel (more accurately sampled than the red and blue ones) and then apply this information to recover the interpolation of the red and blue components (and vice versa). These methods produce an effective improvement of the high-frequencies of the image. However they can introduce zipper effect near the edges degrading the quality of the image.

In this paper we propose a new technique for reducing the artifacts introduced by demosaicing. This approach exploits the high-frequency inter-channel correlation and furthermore avoids to produce zipper effect near the contours of the objects. Section 2 analyzes the causes of the principal errors introduced by demosaicing. In Section 3 the proposed algorithm is described and in Section 4 its performances are discussed. Finally in Section 5 we report the conclusions.

2. ANALYSIS OF THE MOST RECURRENT ERRORS OF DEMOSAICING

As seen in Section 1, many demosaicing techniques have been proposed in literature and different approaches have been explored. Often the interpolation of the green channel is the first step, since the green component is sampled at a rate twice as high as the red and blue planes and thus possesses most of the spatial information of the image. Moreover, the knowledge of the green image can be useful to reduce the aliasing problem also in the red and blue reconstruction.

It can be noticed that most of the recent algorithms apply the same method to interpolate the green component from the Bayer data. In fact, it is proved [6, 7] that the best technique to interpolate the green channel consists in applying the scheme of Fig. 2, where the downsampled green signal is interpolated with a directional low-pass filter $h_0 = [0.5\ 1\ 0.5]$ and the resulting output is corrected with the mid-frequency

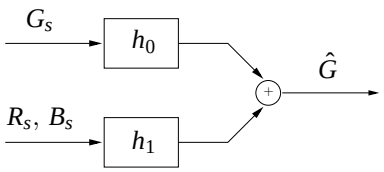

Figure 2: Reconstruction of the green signal.

contribution selected by the filter h_1 applied to the red (or blue) component, which gives the estimate

$$\hat{G}(x) = h_0 * G_s(x) + h_1 * R_s(x). \quad (1)$$

It is found [6, 7] that a good choice for the filter h_1 is the 5-tap FIR $[-0.25\ \ 0\ \ 0.5\ \ 0\ \ -0.25]$ (see Fig. 3). The direction along which the two filters are applied can be selected using an edge-detection estimator as in [5] or, alternatively, the interpolation can be performed both horizontally and vertically and the decision for the best reconstruction is performed afterwards [7–9].

The red and blue components usually are reconstructed using the bilinear interpolation of the color differences $R - \hat{G}$ and $B - \hat{G}$, since the color differences are smoother than the color channels (it is a consequence of the high-frequency correlation between the three color bands).

This approach gives good performance and exploits all the information given by the Bayer pattern. However, it cannot avoid some errors in the reconstruction of the full color image, as can be observed in Table 1 where the Mean Square Errors (MSE) after the reconstruction with some edge-directed demosaicing algorithms are reported. The five test images belong to the Kodak database, also used in [10]. We sampled them according to the Bayer pattern, reported in Fig. 1, afterwards we reconstructed them with different demosaicing techniques, comparing the interpolated images with the original ones. We note that a considerable error is produced in the reconstruction, also with the most demanding algorithms.

There are three principal causes for these reconstruction errors in the interpolation of the green channel:

- a wrong estimation of the direction of the edges. This leads to an incorrect decision for the direction of the filters;
- a local weak correlation in the mid-frequencies between the three color bands. So the term filtered by the filter h_1 and added to the green estimation (see Fig. 2) does not estimate correctly the green mid-frequency value;
- the low-pass characteristic of the filter used to interpolate the green values which is not able to provide the high-frequencies of the image.

Since the estimated green image is used to determine the red and blue components also, these misregistrations could be propagated to the other bands of the image.

This leads to introduce a new step to remove the demosaicing artifacts, as much as possible. Gunturk *et al.* [10] and Li [11] propose two iterative algorithms to recover and improve the interpolated image. However their methods do not use edge information, so they introduce some zipper effect near the contours of the objects, degrading the final quality of the image. Moreover, because of their iterative nature, they are quite computational demanding, especially [10].

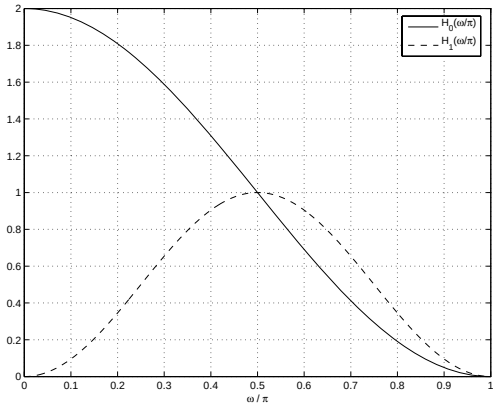

Figure 3: Frequency response of the two filters h_o and h_1.

Test image		Bilinear Interp.	Method [5]	Method [7]	Method [8]
lighthouse	R	129.22	28.89	11.61	12.40
	G	43.44	9.69	7.26	7.73
	B	125.51	28.19	12.97	13.29
sail	R	46.31	11.74	5.56	6.03
	G	17.58	4.56	3.24	3.55
	B	45.70	11.93	5.98	6.60
boat	R	142.34	37.49	12.47	14.10
	G	51.62	15.65	8.13	8.98
	B	135.15	38.25	15.17	17.00
statue	R	46.84	14.36	7.85	8.20
	G	22.73	7.53	5.57	5.80
	B	54.58	17.75	9.34	9.93
window	R	36.18	9.92	5.42	5.77
	G	14.72	3.98	3.35	3.57
	B	37.01	10.63	6.67	7.29
Average	R	80.18	20.48	8.58	9.30
	G	30.02	8.28	5.51	5.93
	B	79.59	21.35	10.03	10.82

Table 1: Mean Square Error (MSE) for some demosaicing algorithms: Bilinear Interpolation, Edge-Directed Interpolation [5], Homogeneity-Directed Demosaicing [7] and Primary-Consistent Soft-Decision Demosaicing [8].

3. DESCRIPTION OF THE PROPOSED REFINING ALGORITHM

3.1 Edge-direction estimation

As said in the previous section, a key issue of many demosaicing techniques is the edge-directed approach. However, when the edge-estimation is performed in a wrong way, it can introduce some annoying artifacts. Thus, we choose a directional approach for our refining algorithm, but, as a first step, we perform an edge-detection that provides a reliable estimation. We apply the *Sobel operator*, a simple and effective tool for edge-detection in grey-scale images [12, 13]. It

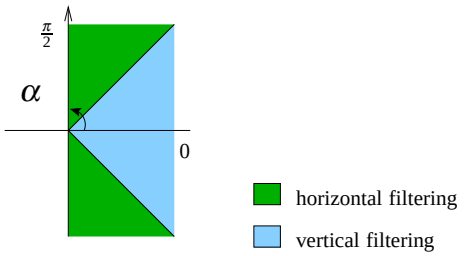

Figure 4: Selection of the directional filtering basing on the values of α.

is based on two masks, defined as:

$$H_x = \begin{bmatrix} -1 & 0 & 1 \\ -2 & 0 & 2 \\ -1 & 0 & 1 \end{bmatrix} \quad H_y = \begin{bmatrix} -1 & -2 & -1 \\ 0 & 0 & 0 \\ 1 & 2 & 1 \end{bmatrix}. \quad (2)$$

When applied to the image, H_x and H_y give an estimate of the first-order partial derivatives along the horizontal and vertical direction, namely A_x and A_y respectively. The gradient of the image f at the pixel (i, j) is defined as

$$\nabla_f(i,j) = \begin{bmatrix} A_x(i,j) \\ A_y(i,j) \end{bmatrix} \quad (3)$$

and its direction is given by

$$\alpha_f(i,j) = \arctan\left(\frac{A_y(i,j)}{A_x(i,j)}\right) \quad (4)$$

where the angle is measured with respect to the x-axis. The direction of an edge is perpendicular to the direction of the gradient vector.

We select two directions for the application of the directional filtering, precisely the two cardinal directions. Therefore the angle α_f has to be rounded and two main states are considered: $\alpha_f \simeq 0$ (for vertical edges) and $\alpha_f \simeq \pm\pi/2$ (for horizontal edges). If $\alpha_f \simeq 0$ the refining is performed vertically, otherwise horizontally, as represented in Fig. 4. Moreover, considering that the arctangent is a monotonically increasing function, the edge-detection can be simplified as follows:

```
if |A_h| > |A_v|
then
  apply vertical filtering
else
  apply horizontal filtering
```

A possible extension of this process of edge-detection consists in considering four principal directions, instead of only two, i.e. selecting also the two cardinal directions associated to $\alpha_f \simeq \pi/4$ and $\alpha_f \simeq -\pi/4$.

While in the demosaicing process a full resolution image is not available for the edge-detection, now we have the three reconstructed components. We choose to perform the edge-detection by applying the Sobel operators over the green image because it is the most reliable reconstructed channel. Since the three color channels are very correlated, they presents similar edges, so the same edge-estimation can be used for all them.

3.2 Refining of the green component

As seen in Section 2, the filters applied to reconstruct the green band can introduce some errors. Furthermore, using the green channel to reconstruct the red and blue colors, these errors are propagated to the other bands. We can correct them by exploiting the inter-channel correlation of the three primary colors. The three reconstructed full-dimension components are used and, moreover, the knowledge of which pixels have been acquired from the sensor according to the Bayer pattern is used.

The first step consists in the correction of the green component, using the edge-direction estimation performed on the image with the Sobel operators. As described in Section 2, some errors derive from the low-pass characteristic of the filters applied in the reconstruction, which do not consider the high-frequency content. However, the lost high-frequency information can be estimated using the high-bands correlation between the colors. In fact, a solution consists in replacing the high-frequency component of each estimated green value with the one of the color of the Bayer-known data at the same pixels. The low-frequency component is preserved unchanged because the low bands are less correlated.

Then, for a pixel at location (i, j), the green value is decomposed as

$$G_{i,j} = G^{\ell}_{i,j} + G^{h}_{i,j}, \quad (5)$$

where $G^{\ell}_{i,j}$ and $G^{h}_{i,j}$ denote the low- and high-frequency components, respectively. Supposing that at this pixel the red value is known from the sensor, also the red value is decomposed into the two components $R^{\ell}_{i,j}$ and $R^{h}_{i,j}$. Then, the green high-frequency value $G^{h}_{i,j}$ is replaced with $R^{h}_{i,j}$ and the green sample is reconstructed as

$$G_{i,j} = G^{\ell}_{i,j} + R^{h}_{i,j}. \quad (6)$$

The correction at pixels where the blue is the known Bayer data is carried out in a similar way. The selection of the low-frequencies is performed using a low-pass filter, while the high-frequencies are calculated subtracting the low-frequency values. The low-pass filter is designed as a 1-dimensional filter, in order to avoid the introduction of artifacts near the edges, and the filter direction is driven by the value of the gradient angles $\alpha_f(i, j)$, as described in Section 3.1. The applied filter is the 3-tap FIR $h_\ell = [1/3\ \ 1/3\ \ 1/3]$ (see Fig. 5).

Another misregistration in the interpolated images can be found in the mid-frequencies due to an incidental wrong effect of the filter h_1 in the scheme of Fig. 2; it is a consequence of the weak correlation between the three bands when there is a wrong selection of the filtering direction. It can be corrected by replacing the mid-frequencies of the green channel with the ones of the red or blue channels along the direction selected with the edge-estimation, as for the correction of the high-frequencies. A good filter to suppress the mid-frequency terms is the FIR $h_m = [1/2\ \ 0\ \ 1/2]$ (see Fig. 5).

We note that the cascade of the two filters h_ℓ and h_m corresponds to a single filter h_u with coefficients $[0.17\ \ 0.17\ \ 0.32\ \ 0.17\ \ 0.17]$ having the frequency response of Fig. 6. Therefore we choose to apply directly the filter h_u on the green image.

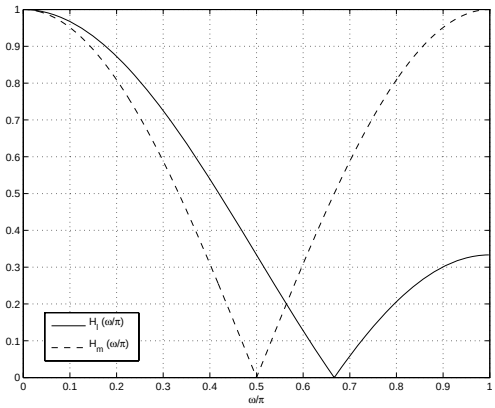

Figure 5: Frequency response of the two filters h_ℓ and h_m.

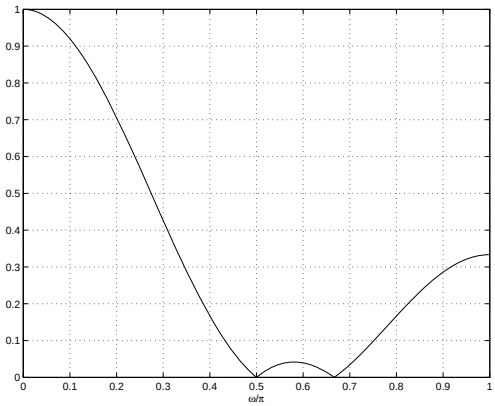

Figure 6: Frequency response of the filter h_u.

3.3 Refining of the red and blue components

After the refining of the green channel, we correct the other color bands. In this case it is experimentally proved that it is more useful to proceed with a different approach with respect to the correction of the green component.

The green pixels (i.e. the pixels where the sensor captured the green values) present only two neighboring red and blue pixels, placed either horizontally, either vertically. Therefore no edge-estimation is used and the correction of the red (blue) values in the green positions is performed using the bilinear interpolation of the color differences $R-G$ ($B-G$) of the pixels where the red (blue) color is known from the Bayer pattern (see Fig. 7).

Instead, in the blue (red) position we have four red (blue) neighboring pixels, placed in the diagonal directions. Interpolating along the diagonal directions can be counterproductive, for two reasons: there is a most relevant presence of cardinal edges in natural images with respect to the other directions, and it is more demanding to implement another edge-direction estimator that detects the diagonal orientations. So, we prefer to perform the correction along the cardinal directions, selected with the edge-detector described in Section 3.1. Once the direction is chosen, a bilinear interpolation of the color difference $R-B$ is carried out; the color difference $R-B$, instead of $R-G$, is preferred in order to exploit the information of the known color value at each pixel. Moreover, the correction of the red (blue) component in the blue (red) pixels follows the refining in the green position, so the values already corrected can be used in order to determine a more reliable color difference.

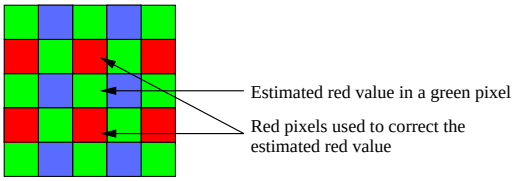

Figure 7: Correction of an estimated red value.

Test image		Proposed refining after			
		Bil. Int.	Meth. [5]	Meth. [7]	Meth. [8]
lighthouse	R	21.20	8.32	6.95	6.95
	G	14.66	5.20	3.86	3.91
	B	22.30	8.93	8.06	7.53
sail	R	8.14	4.78	4.23	4.30
	G	5.40	2.56	2.01	2.06
	B	8.57	5.01	4.57	4.72
boat	R	20.89	10.41	6.56	6.83
	G	14.68	6.98	3.84	4.06
	B	24.20	12.86	9.12	9.66
statue	R	7.50	5.74	5.17	5.12
	G	5.89	3.95	2.95	2.99
	B	8.91	7.08	6.43	6.64
window	R	6.05	5.12	4.95	5.12
	G	3.75	2.63	2.37	2.46
	B	7.15	6.31	6.45	6.68
Average	R	12.76	6.87	5.57	5.66
	G	8.88	4.26	3.01	3.10
	B	14.23	8.04	6.93	7.05

Table 2: MSE between the original images and the resulting ones after the application of the proposed algorithm to the images reconstructed with different demosaicing methods.

4. RESULTS

The Mean Square Errors (MSE) of the interpolated images corrected with the proposed method are reported in Table 2. The algorithm described in the previous section has been applied over the images reconstructed with the techniques presented in [5], [7] and [8]. Comparing the results with the ones of Table 1, where no refining steps have been applied, we can observe that there is a noticeable reduction of the error. In Table 3 the gain (in terms of PSNR) given by the application of the proposed algorithm is reported; it has been computed as difference of the PSNR of the interpolated image before and after the correction step. The improvement of the quality of the image is bigger for the simplest demosaicing techniques (6.92 dB and 3.65 dB for the bilinear interpolation and the edge-directed approach of Hamilton and Adams, respectively), but it is consistent also when the refining step is applied to well-performing methods, such as [7] and [8].

However, a more effective evaluation of the performances is given by a visual inspection of the reconstructed image, because the objective measures, such as MSE and PSNR, often fail to show the subjective quality of the images. An example of the performance of the algorithm is reported in Fig. 8 and other images can be downloaded at

(a) (b) (c)

Figure 8: Portion of image *lighthouse*: (a) original image; (b) image reconstructed with technique [5]; (c) image reconstructed with technique [5] and corrected with the proposed algorithm.

Test image	With Bil. Int.	With Meth. [5]	With Meth. [7]	With Meth. [8]
lighthouse	6.69	4.37	2.35	2.65
sail	6.65	3.39	1.48	1.76
boat	7.09	4.60	2.75	3.02
statue	7.23	3.59	2.07	2.22
window	6.95	2.31	0.68	0.84
Average	6.92	3.65	1.86	2.10

Table 3: PSNR gain (in dB) given by the application of the proposed algorithm over the images reconstructed with different demosaicing techniques.

http://www.dei.unipd.it/ntrda. It can be noticed that the proposed method reduces the demosaicing artifacts and, moreover, due to the directional approach, does not introduce zipper effect near the edges.

5. CONCLUSION

In this paper we presented a new approach for reducing the artifacts introduced by the interpolation of images captured with the Bayer pattern. It improves the final quality of the reconstructed images and can be applied after different demosaicing techniques. The best results are achieved when the interpolation has been performed in a fast way but a significant improvement is also given with well-performing techniques. Moreover, the computational cost of this algorithm is low and no iterations are required, allowing for an implementation in the digital cameras, or alternatively as a post-processing tool.

Acknowledgement

The authors would like to thank K. Hirakawa for providing the software of his algorithm.

REFERENCES

[1] B. E. Bayer, "Color imaging array," U.S. Patent 3 971 065, July, 1976.

[2] B. K. Gunturk, J. Glotzbach, Y. Altunbasak, R. W. Schafer, and R. M. Mersereau, "Demosaicking: color filter array interpolation," *IEEE Signal Processing Mag.*, vol. 22, pp. 44–54, Jan. 2005.

[3] D. R. Cok, "Signal processing method and apparatus for producing interpolated chrominance values in a sampled color image signal," U.S. Patent 4 642 678, Feb., 1987.

[4] C. A. Laroche and M. A. Prescott, "Apparatus and method for adaptively interpolating a full color image utilizing chrominance gradients," U.S. Patent 5 373 322, Dec., 1994.

[5] J. F. Hamilton and J. Adams, "Adaptive color plane interpolation in single sensor color electronic camera," U.S. Patent 5 629 734, May, 1997.

[6] J. E. Adams, "Design of practical color filter array interpolation algorithms for digital cameras, part 2," in *IEEE Proc. Int. Conf. Image Processing*, vol. 1, Oct. 1998, pp. 488–492.

[7] K. Hirakawa and T. W. Parks, "Adaptive homogeneity-directed demosaicing algorithm," *IEEE Trans. Image Processing*, vol. 14, no. 3, pp. 360–369, Mar. 2005.

[8] X. Wu and N. Zhang, "Primary-consistent soft-decision color demosaicking for digital cameras (patent pending)," *IEEE Trans. Image Processing*, vol. 13, no. 9, pp. 1263–1274, Sept. 2004.

[9] N. Zhang and X. Wu, "Color demosaicking via directional linear minimum mean square-error estimation," *IEEE Trans. Image Processing*, vol. 14, no. 12, pp. 2167–2177, Dec. 2005.

[10] B. K. Gunturk, Y. Altunbasak, and R. M. Mersereau, "Color plane interpolation using alternating projections," *IEEE Trans. Image Processing*, vol. 11, no. 9, pp. 997–1013, Sept. 2002.

[11] X. Li, "Demosaicing by successive approximation," *IEEE Trans. Image Processing*, vol. 14, no. 3, pp. 370–379, Mar. 2005.

[12] A. K. Jain, *Fundamentals of digital image processing*. Prentice Hall, 1989.

[13] R. C. Gonzalez and R. E. Woods, *Digital Image Processing*, 2nd ed. Prentice Hall, 2002.